Polymer Bulletin
https://doi.org/10.1007/s00289-022-04311-1

ORIGINAL PAPER

Fabrication and evaluation of electrospun polyacrylonitrile/silver nanofiber membranes for air filtration and antibacterial activity

Majid Sohrabi[1] · **Marjan Abbasi**[1] · **Asghar Sadighzadeh**[2]

Received: 3 February 2022 / Revised: 23 May 2022 / Accepted: 30 May 2022

Abstract

Particulate matter and airborne microorganisms are two of the most severe indoor air problems due to their significant risks to human health. Comprehensive research on air filtration with good filtration performance for fine particles and antibacterial function is essential. In this study, after some experimentations and optimization of conditions, polyacrylonitrile (PAN) 10–1% silver nanoparticles (AgNPs) membranes with suitable morphology and uniform diameter distribution are fabricated by an electrospinning method. These electrospun mats exhibited antibacterial activity toward *Staphylococcus aureus* (Gram-positive bacteria) and *Escherichia coli* (Gram-negative bacteria). With its small pore size, high porosity, the high specific surface area of 42 m^2/g, and robust mechanical strength of 7.14 MPa properties, the resultant PAN10%-1%Ag membranes exhibit high filtration efficiency of 99.27%, the low pressure drop of 33 Pa, and higher quality factor compared to the two standard commercial masks including, the three-ply surgical mask and the respirator face mask. After 24 h of the filtration process in a simulated living environment, the obtained air filter still displayed a high filtration efficiency and a less pressure drop variation. In addition, the R^2 value was 0.99, which indicates that the calculation results are in good agreement with the measured results. The fabrication of PAN-Ag membranes will have broad applications, including face masks, indoor air filtration and clean room.

Keywords Nanofibers · Electrospinning · Air filtration · Antibacterial activity · Membrane

✉ Marjan Abbasi
m.abbasi@guilan.ac.ir

[1] Department of Textile Engineering, Faculty of Engineering, University of Guilan, Rasht, Iran

[2] Plasma Physics and Nuclear Fusion Research School, Nuclear Science and Technology Research Institute, AEOI, Tehran, Iran

Published online: 29 June 2022

Introduction

People spend a lot of time in buildings, and indoor air quality (IAQ) is tightly related to people's health, work and even lives. Particulate matter (PM) and airborne microorganism have attracted more attention following the increasing trend of severe environmental problems, due to the increased emissions of automobile exhaust and industrial air, as well as frequent sandstorm accidents [1].

Technically, PM2.5 refers to particulate matter 2.5 μm or less in diameter. PM2.5 and submicron particles are noticeably harmful and can migrate to the human lungs or in some cases to other organs of the body, thus increasing respiratory and cardiac morbidity [2, 3]. PM2.5 is combined with organic matter (organic carbon and elemental carbon) and inorganic components (such as SiO_2, SO_4, and NO_3) [4, 5].

Air filtration technology (such as stretched membrane filtration, electrostatic capture filtration and fiber filtration) can play an essential role in improving IAQ and protecting human health; it can be captured PM and airborne microorganisms simultaneously [6]. In order to protect human health, various air purification products have been produced. However, filters based on conventional fibers (such as melt-blown fibers, spun-bonded fibers and glass fibers) do not meet the demand of air purification, especially for the removal of fine particles with a diameter in the range of 300–500 nm suspended in the atmosphere [7–9]. Additionally, the airborne microorganism that is intercepted on the surface of the fibrous air filters does not die but can multiply under suitable conditions of temperature and relative humidity. If the filter is broken, the microorganisms will enter the indoor environment [10]. Generally, the systematic design of membranes for the purification of fine particles requires the consideration of two important rules: (1) packing density, in which a large intra-fiber void can lead to the penetrate of air flow across the membranes, so that prevent the penetration of fine particles and (2) the fiber diameter, which affects the capturing efficiency of hazardous particles by the membranes [11–13]. Theoretical predictions have shown that nanofibers with a diameter of less than 500 nm, there will be a slip flow effect, which is suitable for simultaneous low air resistance and high filtration efficiency with respect to traditional microfibers [14, 15]. Also, the high specific surface area of nanofibers can improve filtration efficiency compared to microfibers.

At present, various methods have been developed for the fabrication of nanofiber-based membranes for the separation of fine particles, including template synthesis, phase separation, melt-blown method, and plasma treatment [16–20]. Unfortunately, most of these methods still suffer from relatively low filtration efficiencies and high energy consumption and are also unsuitable for practical applications due to their low stability and poor reusability.

As we all know, electrospinning is known a simple and effective technique for fabricating polymer nanofibers [21]. Polymer nanofibers have attracted the attention of many researchers in recent decades due to their high specific surface area, small pore size and special features that are interesting in advanced applications [22–24]. Electrospun nanofibers have potential applications in tissue engineering

scaffolds [25], air filters [26, 27], wound dressings [28], drug delivery materials [29], electronics [28], and catalytic carriers [30], among others.

Polymeric solutions or melts have been fabricated the fibrous membranes through electrically charged jets. Although nanofiber membranes have been widely used as air filters, many of their problems such as low filtration efficiency, high resistance and short service life still exist. All of this can be attributed to the limited structural control of thick-diameter fibers (not real nanoscale of < 100 nm) and their easy-collapsed cavity structure and stop the widespread use of these membranes [31, 32]. Many parameters, such as fiber diameter, pore size distribution, porosity and nanostructure or microstructure of fiber membranes, affect the filtration performance of nanofiber membranes [33, 34].

The properties of nanofiber filters are usually determined by PM removal efficiency and pressure drop, which are calculated conforming to the particle concentrations and the pressure difference between the upstream and downstream of the filter [35]. It is usually assumed that the removal efficiency is done at the cost of reducing air permeability due to the tightened of the filter structure and the deposition of the PM on the filter. As a result, many efforts have been assigned to increase the removal efficiency filter without losing air permeability [36–38]. Since the removal efficiency of a filter is determined by both morphology and inherent chemical properties of the nanofibers, it is critical to establish a suitable structure and select an appropriate material. Many polymers, including polyacrylonitrile (PAN), polyvinyl acetate (PVA), polypropylene (PP), polystyrene (PS), polyvinyl pyrrolidone (PVP), etc., have been electrospun as air filters [39–42]. Among these polymers, the PAN nanofibrous membranes are often used as the filtration mediums because of their excellent thermal and chemical stabilities. Besides, the induced-dipole and dipole–dipole forces of PAN are able to increase the interaction between PMs and nanofibers and attain the highest PM removal efficiency [39]. The continuous use of the filter media exposes them to attacks by environmental microorganisms. These microorganisms captured by the filter proliferate, leading to the formation of biofilms that worsen the quality of the filtered air. The use of antibacterial material over the filter provides a solution to the above problem [43, 44].

The objective of this study is to evaluate and develop a composite filter made of polyacrylonitrile (PAN) nanofibers with incorporated silver (Ag) nanoparticles on polyethylene terephthalate (PET) nonwoven fabric mesh. Also, the morphology, pore structure, mechanical properties, filtration performance and antibacterial activity of nanofiber membranes have been carefully investigated and a filtration simulation based on pore structure has been proposed.

Experimental section

Materials

PAN powders (Mw = 90,000) were purchased from Spectrum Chemicals and Laboratory Products Co., Ltd., USA. N,N-Dimethylformamide (DMF) was obtained from Shanghai Chemical Reagents Co., Ltd, China. Silver nitrate (MW 169.88 g/mol) was

purchased from SRL chemicals, India. The traditional Three-Ply surgical mask and respirator face mask (80 g/m^2), as two kinds of Standard face mask, were purchased from the commercial market. A three-ply surgical mask (also known as a surgical mask) is composed of 3 layers of synthetic nonwoven materials (Polypropylene), configured to have a filtration layer sandwiched in the middle, available in 1.24 mm thicknesses and 0.63 kPa.s/m air resistance. The respirator face mask is a respiratory protective device designed to achieve a very close facial fit and efficiently filtration of airborne particles. Note that the edges of the respirator are designed to form a seal around the nose and mouth. The respirator face mask is made of synthetic nonwoven materials (Polypropylene); available in 2.42 mm thicknesses and 1.56 kPa.s/m air resistance. The polyethylene terephthalate (PET) nonwoven fabric mesh with negligible filtration capacity (filtration efficiency of ~3.5% and pressure drop of ~0.5 Pa for 300 nm particles under the face velocity of 32 L/min) for fiber receiving was purchased from the commercial market. All chemicals were used without further purification.

Preparation of nanofiber membranes

10 wt% (note that wt1% is equal to 1 g of PAN powders in 100 g of DMF) solutions were prepared by dissolving PAN in DMF with a magnetic stirring process for 24 h at room temperature. The fabrication of nanofibrous membranes was performed by using the DXES-3 spinning equipment (Shanghai Oriental Flying Nanotechnology Co., Ltd., China).

Typically, homogeneous solutions are loaded into 5-ml plastic syringes and injected through 24-gauge metal needles at a feed rate for electrospinning. The stainless-steel roller covered with a non-woven polyethylene terephthalate substrate rotates at a speed of 80 rpm and keeps a tip-to-collector distance of 20 cm. In order to ensure the uniformity of properties in nanofiber membrane, which include thickness and basis weight, we placed a plastic syringe on the injection pump, which horizontally traveled backward and forwards with the speed of 250 cm/min within a fixed distance using a mechanical slide unit. During the electrospinning process, flow rates of PAN were controlled at 0.2 ml/h, by a peristaltic pump. The high voltage applied to the needle of the PAN solutions syringe was 18 kV and the relevant temperature and humidity were 25 ± 2 °C and 33 ± 2%, respectively. All samples were vacuum-dried at 70 °C for 1 h to remove the residual solvent and charges. The schematic of the experimental setup is shown in Fig. 1.

Characterization and measurements

The morphology of the composite membranes was examined by field emission scanning electron microscopy (FESEM; S-4800, Hitachi Ltd, Japan). The fiber diameters in the membrane were measured at 50 different points by the image analyzer (digimizer software).

Antibacterial activity of PAN-AgNPs electrospun membranes was investigated by the zone inhibition method. All PAN-AgNPs electrospun membranes with different

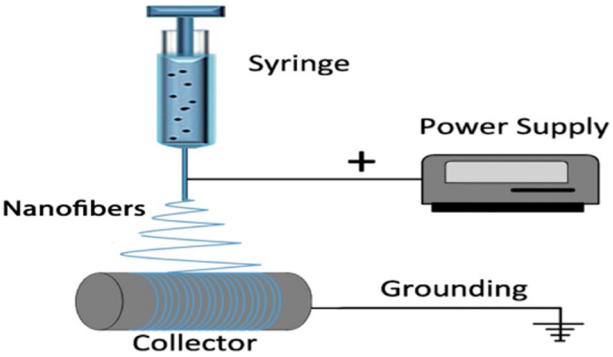

Fig. 1 Schematic showing the fabrication of PAN-AgNPs electrospun nanofibers on the collector drum

contents of AgNPs were cut into 6 mm diameter circular disks and sterilized by UV light prior to the bacterial viability test. *Staphylococcus aureus* (Gram-positive bacteria) and *Escherichia coli* (Gram-negative bacteria) were chosen as model microorganisms in this study. Then, nanofibers disks were transferred to *Staphylococcus aureus* or *Escherichia coli* bacterium suspension containing around 106 colony forming units (CFUs)/mL and incubated for 24 h at 37 °C. Zones of inhibition were measured by testing the diameter of the inhibition area around each disc.

The Fourier transform infrared spectra of the membranes were obtained using a Paragon 1000 Spectrometer (Perkin Elmer) at a signal resolution of 1 cm^{-1} within the range of 400–4000 cm^{-1}; the thickness of membranes was measured by a microscrewmeter (0–25 mm, Shanghai).

The mechanical properties of the different samples were measured with a testing machine (Instron 3345, single column, UK) at a crosshead speed of 20 mm/min at room temperature. The membranes tested had a length of 30 mm and a width of 5 mm.

The contact angle of the membrane with a drop of water (3 µL) was measured by a contact angle analyzer (Kino Industry Co., Ltd., USA). To measure the mechanical properties of the material at least 10 samples have been tested. The average results of the tensile strength, elongation at the break and tensile modulus were reported. The contact angle of the membrane with a drop of water (3 µL) was measured by a contact angle analyzer (Kino Industry Co, USA). To benefit the authenticity of the test results, the contact angle was measured ten times, and the average of the values was recorded.

The surface areas of the pure PAN were measured by a surface area tester (KuBo-X1000, Beijing Builder Technology Co., Ltd., China). The pore size and pore size distribution of electrospun membranes were analyzed by pore size meter (PSM-165, Topas, GmbH, Germany).

The schematic of the filtration process is shown in Fig. 2. Atmospheric aerosol was used as experimental particles. A pump (Model DING HWA Co) assures the air circulation in the device. The upstream and downstream aerosol concentration was determined by a condensation nucleus particle counter (Model 5.412, GRIMM Co). The

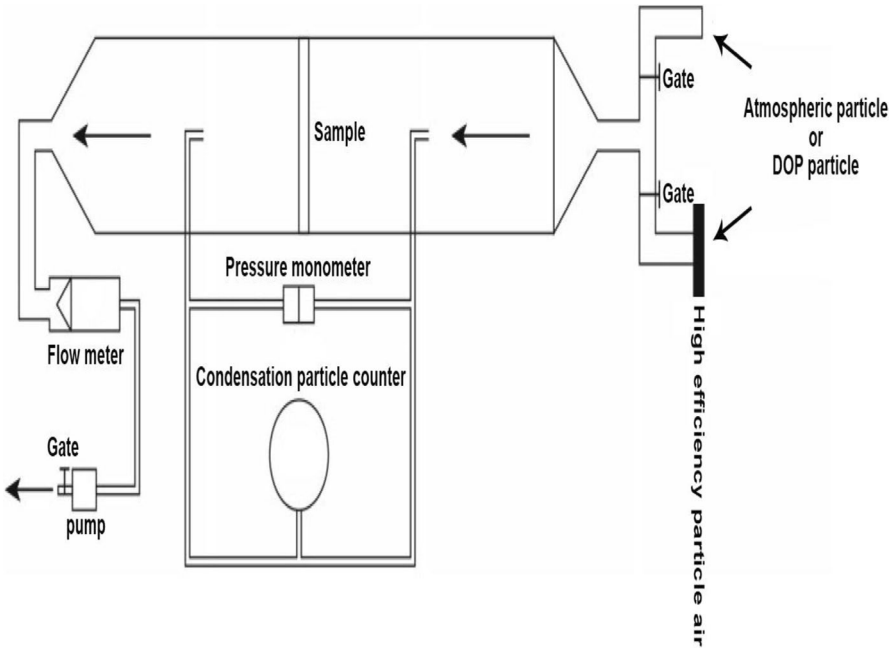

Fig. 2 Schematic of filtration process

membrane pressure drop was obtained by a pressure manometer device (Model 202, KIMO Co). At the beginning of all tests, the air in the system is filtered by a high efficiency particle air (HEPA) filter in order to ensure no leakage in the system by measuring the concentration of aerosol particles upstream and downstream of the sample. 2 wt% NaCl aqueous solution was employed to generate the NaCl aerosol particles using the QRJ-1 NaCl atomizer. 300,000–500,000 Charge-neutralized monodisperse solid sodium chloride (NaCl) aerosol particles (charge neutralized by electrostatic neutralization device), with mass mean diameter of 50–500 nm and geometric standard deviation less than < 1.86, were released through the membrane, which was pinned by a filter holder with an effective area of 100 cm^2. Then, the number of NaCl particles in the upstream and downstream of the airflow can be accurately measured via the condensation nucleus particle counter, and the filtration efficiency is calculated via the data processing system. Similarly, the air resistance can be examined by the manometer that might detect the air pressure before and after the filter under a controlled airflow velocity. For the long-term test that simulated a practical living environment, the entire test was conducted for 24 h continuously to study the long-term performance of the fabricated PA-6 NFN membranes.

Results and discussion

Morphology, zone of inhibition and properties of the PAN-AgNPs membrane

The goal of this work is to fabricate a high-performance composite filter made of PAN nanofibers with incorporated silver (Ag) nanoparticles for air filtration and good antibacterial function. Optimizing the membrane design to achieve the highest filtration performance of fine particles requires the creation of membranes with a small fiber diameter and low packing density. The SEM images for PAN nanofibers membranes with 0, 0.5, 1 and 2 wt.% Ag nanoparticles are shown in Fig. 3a–d, which shows the distribution of nanofiber diameters. From Fig. 3, it is determined that the nanofibers are randomly arranged with a uniform diameter. There are no droplets or beads on the surface of the fibers, indicating that the electrospinning parameters have been selected logically in this study. In nanofibrous membranes, a three-dimensional porous structure is observed due to a large number of pores between fibers.

In Fig. 3(a), when Ag does not exist, the average diameter of the nanofibrous membrane is 320 nm with a distribution of 49 nm. In Fig. 3b–d, the average diameter of fibers changes slightly by increasing the antibacterial agent content and the diameter distribution of nanofibers is uniform, but their average diameter is higher than the nanofibrous membrane that has no antibacterial material. Nevertheless, the surface of modified fibers such as fibers without adding Ag is smooth and no drops or rosary seeds are observed in it.

AgNPs by releasing Ag^+ to attack the respiratory chain, cell division leads to bacterial cell death [45].

Furthermore, the high surface area of AgNPs can provide great action sites for microorganisms to raise bactericidal activity.

The antibacterial property of PAN-AgNPs with different contents of AgNPs (0, 0.5, 1 and 2 wt%) against *Escherichia coli* and *Staphylococcus aureus* as shown in Figs. 4 and 5 performed by the disk diffusion susceptibility test after 24 h incubation. The diameter of inhibition zone for each sample is recorded in Table 1. As observed in the zone of inhibition data, Pristine PAN the diameter of the inhibition zone for pure PAN is 6.0 mm and no change was observed in the pure PAN membranes antibacterial efficiency (the diameter of the cut disks of the membranes for inhibition zone test is 6 mm). The inhibition zones of PAN-AgNPs (0.5, 1.0 and 2.0 wt%) against Escherichia coli were 7.05 ± 0.3, 8.45 ± 0.9 and 7.35 ± 0.5 mm, respectively.

Furthermore, PAN-AgNPs (0.5 and 1.0 wt %) was exhibited to inhibit the growth of bacteria with slightly higher effectiveness against *Staphylococcus aureus* compared with *Escherichia coli*. The zones of inhibition increased to 7.61 ± 0.1 and 9.51 ± 0.4 mm, which indicating Gram-positive bacteria might be more sensitive to silver antibacterial agents than Gram-negative bacteria. It was mentioned that the most antibacterial affected both two microorganisms when PAN-1%Ag was loaded to PAN electrospun membranes. After adding more AgNPs, the antibacterial property of PAN electrospun membranes weakened

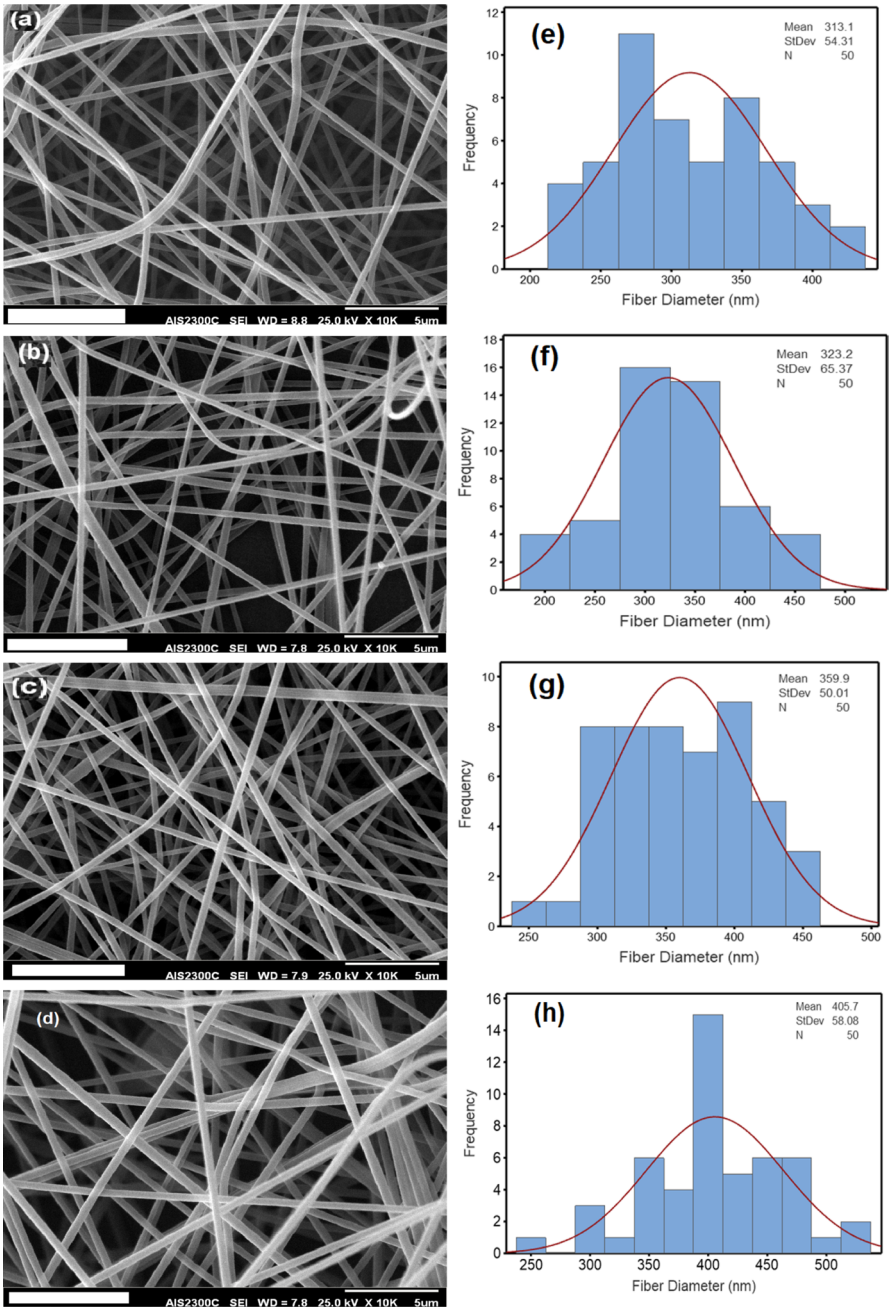

Fig. 3 SEM images and fiber diameter distribution of nanofibers; **a** and **e** PAN 10%, 0% Ag; **b** and **f** PAN 10%, 0.5% Ag; **c** and **g** PAN 10%,1% Ag; **d** and **h** PAN 10%, 2% Ag. The red lines show the approximate distribution based on a Gaussian distribution

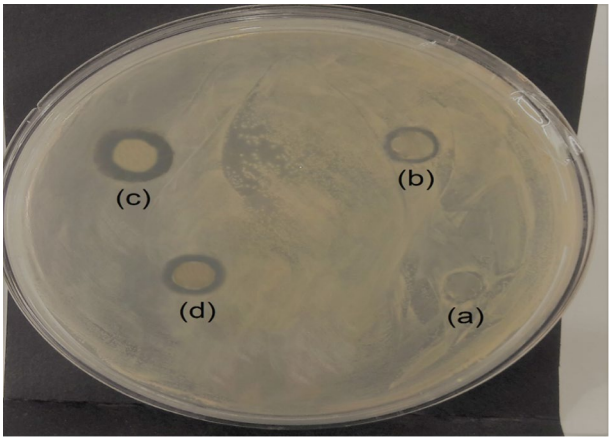

Fig. 4 Photograph showing zone of inhibition of the PAN-Ag membranes against *Escherichia coli* included **a** Ag 0.0%, **b** Ag 0.5%, **c** Ag 1.0% and **d** Ag 2.0%

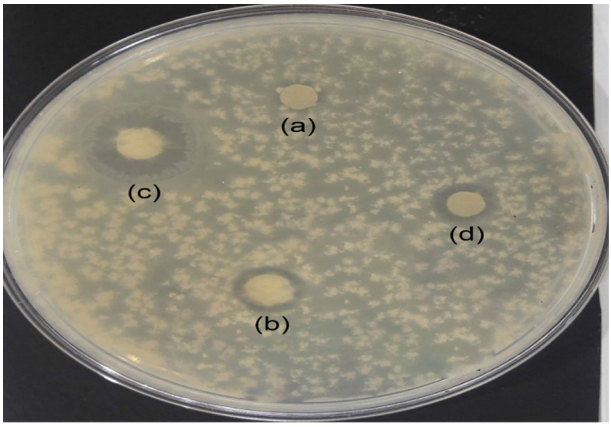

Fig. 5 Photograph showing zone of inhibition of the PAN-Ag membranes against *Staphylococcus aureus* included **a** Ag 0.0%, **b** Ag 0.5%, **c** Ag 1.0% and **d** Ag 2.0%

Table 1 The diameter of inhibition zones of PAN-Ag electrospun nanofibers against *Escherichia coli* and *Staphylococcus aureus*

Sample	*Escherichia coli* (Gram−) inhibition zone (mm)	*Staphylococcus aureus* (Gram+) Inhibition zone (mm)
Ag 0.0	6.0 ± 0.0	6.0 ± 0.0
Ag 0.5	7.05 ± 0.3	7.61 ± 0.1
Ag 1.0	8.45 ± 0.9	9.51 ± 0.4
Ag 2.0	7.35 ± 0.5	7.74 ± 0.2

mainly owing to the potentially devastating effects of AgNPs and to the aggregation of AgNPs at relatively high concentrations [45].

Therefore, this study evaluates the properties and filtration performance of PAN10%-1% Ag, which can be used as excellent materials in air filtration applications.

The Fourier transform infrared (FTIR) has been used to investigate the effect of adding silver on the surface of the PAN membrane. Most of the peaks observed in the two samples are similar with minor differences. This indicates that the addition of 1% silver does not have a significant effect on bonding in PAN and PAN-AgNPs.

The characteristic transmittance peaks of the PAN and PAN-AgNPs membranes can be assigned as shown in Fig. 6: showed no change in the C ≡ N bond with the addition of silver by the characteristic peak of PAN at 2242 cm^{-1} (assigned to C ≡ N) [46–48]. Thus, the possibility of the formation of coordination bonds between PAN and silver was negligible [48]. The bending and stretching vibrations of the $C–H_2$ functional group in PAN, are displayed by the peaks at 1451 and 2920 cm^{-1}, respectively [45, 49]. Because of PAN oxidation in air, the peak at 1745 cm^{-1} is assigned to C = O [45, 49]. The peaks at 536 cm^{-1} and 1745 cm^{-1} are assigned to C = O bending and C = O stretching [49]. The peaks at 1250 cm^{-1} and 1357 cm^{-1} are assigned to CH group vibrations of CH and CH_2, respectively [47].

The characteristic FTIR spectrum confirms most of the peaks observed in the two samples are similar with minor differences. This indicates that the addition of 1% silver does not have a significant effect on bonding in PAN and PAN-AgNPs. Other properties of PAN-1%Ag membrane are listed in Table 2.

The result of the pore structure analysis offered a deep explanation for this sieving manner. As shown in Fig. 7, the PAN10%-1%Ag electrospun membranes possessed a wide pore distribution ranging from 0.3 to 0.9 μm with a mean pore size of 0.62 μm, which was suitable for intercepting the > 0.3 μm particles without obviously sacrificing its air permeability.

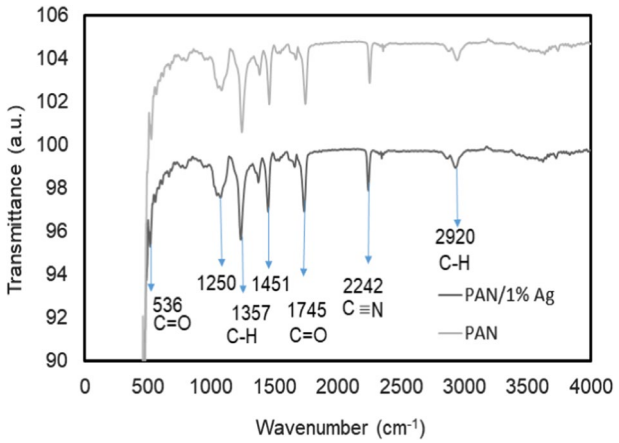

Fig. 6 Comparison of FTIR spectra of PAN and PAN-1%Ag membranes

Table 2 Some properties of PAN-1%Ag electrospun nanofibers

Tensile strength (MPa)	Elongation at the break (%)	Tensile modulus (MPa)	Contact angle (°)	BET surface area (m^2/g)
7.14	31.73	119.45	146	42.46

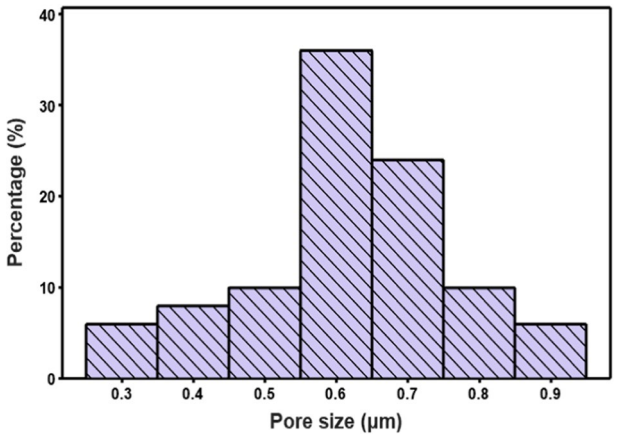

Fig. 7 Pore size distribution of PAN-1%Ag

In general, the mechanical properties of membranes in severe operating conditions such as high air flow and working pressure have some weaknesses in filtration applications. The PAN10%-1%Ag electrospun membranes fabricated at 10 wt % exhibited a relatively high tensile strength of 7.14 MPa, an elongation at break value of 31.73%, and a tensile modulus of 119.45 MPa.

The mechanical properties result of PAN10%-1%Ag shows the resulting membrane has an excellent mechanical property compared to similar nanofibers and has the ability to be applied in air filtration applications [50].

The contact angle of the PAN10%-1%Ag was 146°, which indicates the hydrophobic nature of the membrane, which originates the PAN relatively hydrophobic nature and nano-scaled rough structures imparted by Ag. This prominent wettability was remarkably better than that of commercial PP nonwoven filter media (usually exhibit hydrophobicity behavior), which makes the PAN10%-1%Ag membrane a good candidate for the antifouling fibrous filter media [8, 51].

Generally, the membrane specific surface area is related to its adsorption capacity and the adsorption capacity of the resulting membrane increases with the expansion of specific surface area. The BET surface area of the PAN10%-1%Ag was calculated 42.46 m^2/g, which indicated an obvious increase in the relevant surface area compared to other electrospun nanofibers membranes in similar researches [52, 53]. The reason seems due to the increase in surface roughness originated the presence of silver nanoparticles and small fiber diameter in the resulting membrane.

Filtration performance evaluation

The overall filtration performance of the PAN10%-1%Ag membrane with different basis weights under the industrial standard air flow of 32 L/min, is shown in Fig. 8a. The filtration efficiency of PAN10%-1%Ag membrane against the gained basis weight of 0.25, 0.5, 0.75, 1, 1.25,1.50, 1.75 and 2 g/m^2, was 39.12%, 62.65%, 83.78%, 91.25%, 95.44%, 98.12, 98.59 and 98.76%. Additionally, the related pressure drops were 6, 8, 14, 21, 25, 29, 36 and 43 Pa, respectively. The gained basis weight, was prepared by extending electrospinning time.

Obviously, the filtration efficiency shows a significant increase and then reaches an almost steady state when the basis weight reaches 1.50 g/m^2. Therefore, it can easily attain the standard of N95 filters (> 95%) when the basis weight reaches 1.50 g/m^2 and higher, which is not available for conventional filters.

Considering the proportionality between filtration efficiency and pressure drop, it seems that PAN10%-1%Ag nanofibers with a basis weight of 1.50 g/m^2 are the most suitable options for selecting optimal nanofibers, which are used in other air filtration tests.

To demonstrate the outstanding properties of PAN10%-1%Ag membrane, further investigations were performed on the filtration properties. For this purpose, filtration efficiency and quality factor of different particle sizes were evaluated. On the other hand, pressure drop of filters under different face velocities was analyzed. In the study of filtration properties, samples of a conventional three-ply surgical mask, respirator face mask and the PAN10%-1%Ag medium were used for comparison, as shown in Fig. 8b–d.

As can be seen in Fig. 8b, the filtration efficiency of these three kinds of filters mentioned above showed almost similar behavior while increasing the particle size. In all three filters, it was observed that as the particle size increases, the filtration efficiency first decreases to reach the minimum filtration efficiency and then increases. Nevertheless, it is interesting to note that PAN10%-1%Ag is more effective in trapping the particles. The filtration efficiency is 99.27%, 84.81% and 95.27% for the 100,300 and 500 nm aerosol particles, while the filtration efficiency for the Respirator Face Mask is 86.15%, 82.01% and 88.18% and in Three-Ply surgical mask is 52.11%, 47.85% and 54.75% in 100,300 and 500 nm aerosol particles, respectively. The higher filtration efficiency in PAN10%-1%Ag compared to the other two membranes seems to be related to small fiber diameter and small pore size of PAN-Ag membrane that improved filtration efficiency based on the physical sieving manner. Therefore, PAN10%-1%Ag membrane has a more remarkable ability to remove aerosol particles. It should be noted that the filtration efficiency of filters in 100 nm aerosol particles is important, because the diameter of viruses included in SARS-CoV-2 is about 100 nm. Therefore, it could be concluded that filters with high filtration efficiency in 100 nm aerosol particles are effective against airborne particles including of viruses.

Under experimental conditions, the air flow in the medium is usually a low Reynolds number regime (Re < 1), so the Stokes flow regime prevails in all three membranes. This shows that Darcy's law governs viscous resistance in which the

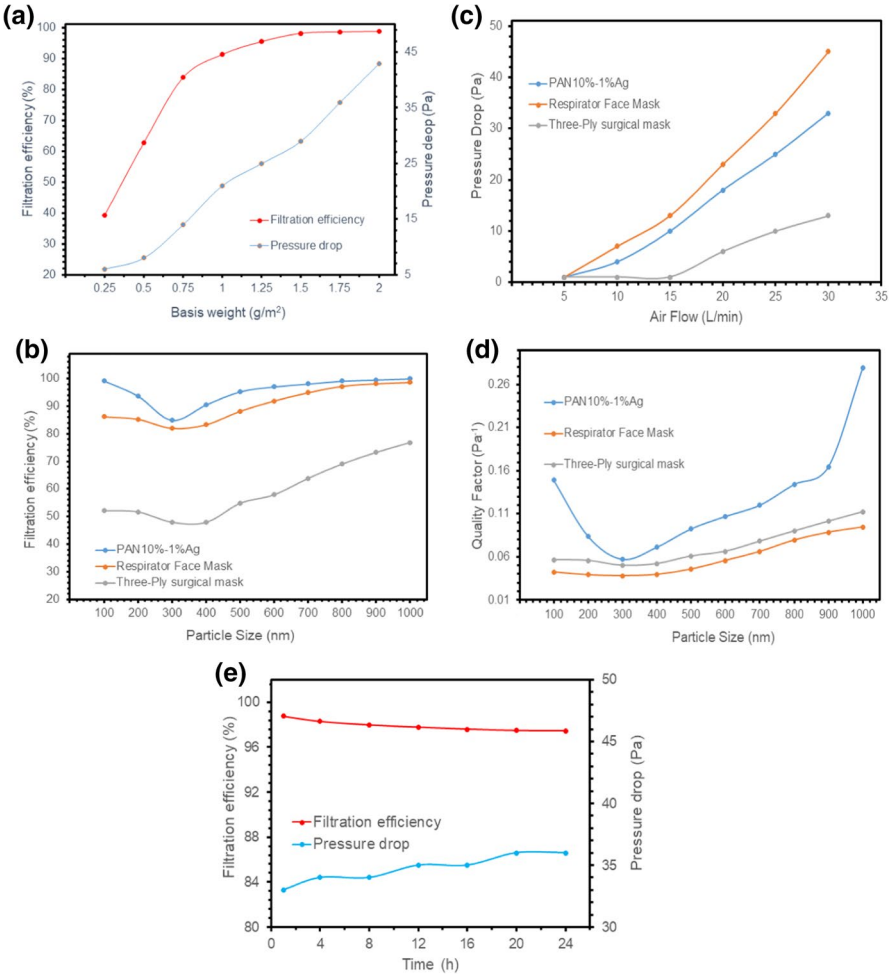

Fig. 8 **a** Filtration performance of PAN10%-1%Ag membrane with various basis weight. **b** Filtration efficiency of PAN10%-1%Ag (1.50 g/m^2), Respirator Face Mask and Three-Ply surgical mask in various particle size. **c** Pressure drop versus face velocity of the PAN10%-1%Ag (1.50 g/m^2), respirator face mask and Three-Ply surgical mask with 100 nm particle size of aerosol. **d** Quality factor of PAN10%-1%Ag (1.50 g/m.^{2}), Respirator face mask and three-ply surgical mask in various particle size and **e** the filtration efficiency and the pressure drop of the PAN10%-1%Ag membrane after 5 filtration cycles

pressure drop is directly proportional to the face velocity [8], which is consistent with experimental results obtained in this article.

Figure 8c shows the pressure drop versus face velocity curves, the slope of which can be used to assess the air permeability of filters.

Compared to the other two filters, the slope of the PAN10%-1%Ag membranes was 1.32, which is higher compared to Three-Ply surgical mask) the slope is 0.52) and lower compared to Respirator Face Mask (the slope is 1.76).

The trade-off parameter of quality factor (QF) values different aerosol particle sizes in Fig. 8d that could be determined by the following equation to exhaustively assess the filtration performance of the PAN10%-1%Ag membrane was presented.

$$\mathrm{QF} = -\ln(1-\eta)/\Delta P \tag{1}$$

where η and ΔP represented the filtration efficiency and pressure drop, respectively [51, 54]. Filter with a better filtration performance should have a higher efficiency and higher QF.

It is observed that QF of PAN10%-1%Ag membrane is better in contrast to other filtration media, which could be attributed to small fiber diameter, small pore size and high porosity of resulted nanofiber structure, showing the more effective application of this filter against airborne pollutants and SARS-CoV-2 and great application potential in the energy saving society.

Figure 8e shows that the PA-6 NFN membrane still maintains a high filtration efficiency ($98.76 \pm 0.62\%$) and less variation of pressure drop (33 ± 3 Pa) after 24 h of operation of the filtration process, fully indicating their robust adaptive capacity and long lifetime for a variety of practical applications.

Theoretical calculation of filtration efficiency and comparison with experimental results

In order to evaluate the theoretical calculation, experimental measurement and to determine their agreement, the equations related to filtration efficiency must first be mentioned.

The total filter efficiency η can be expressed as a function of the single fiber efficiency η_s, filter thickness Z, fiber packing density α, and the fiber diameter d_f [55],

$$\eta = 1 - \exp\left(-\frac{4\alpha\eta s Z}{\pi(1-\alpha)\mathrm{df}}\right) \tag{2}$$

The mechanical capture is through interception (aerosol followed by streamline which gets intercepted by fiber) and diffusion (random walk) with respective single-fiber efficiency for interception η_R and diffusion η_D. The mechanisms of inertia effect, electrostatic effect and gravity effect are ignored here. Assuming these are independent mechanism, the total single fiber efficiency is [55]:

$$\eta s = \eta_R + \eta_D \tag{3}$$

The single fiber efficiency for interception is given by [55]:

$$\eta_R = 0.6\left(\frac{1-\alpha}{\mathrm{KU}}\right)\left(1 + \frac{\mathrm{Kn}_f}{D_p/d_f}\right)\left(\frac{D_p^2/d_f^2}{1 + D_p/d_f}\right) \tag{4}$$

where the aerosol particle diameter to the fiber diameter Dp/df is the interception ratio.

The theoretical single fiber efficiency for diffusion is given by [52]:

$$\eta_D = 1.6\left(1 - \frac{\alpha}{\mathrm{KU}}\right)^{-1/3} \mathrm{pe}^{-\frac{2}{3}} C_1 C_2 \tag{5}$$

where $\mathrm{KU} = -\left(\frac{\ln \alpha}{2}\right) + \alpha - \frac{\alpha^2}{4} - \frac{3}{4}$ is the Kuwabara's hydrodynamic coefficient, and.

$\mathrm{Pe} = U_0 \frac{\mathrm{df}}{D}$ is the Peclet number. U_0 is the face velocity, $D = K_B \frac{TC_S}{3\Pi\mu D_p}$ is the diffusion coefficient, $C_S = 1 + Kn_p\left[1.207 + 0.44e^{(-0.78/Kn_p)}\right]$ is the slip correction factor,

$Kn_p = 2\lambda/D_p$ is the Knudsen number, $\lambda = 65.3$ nm is the air mean free path.

$K_B =$ is the Boltzmann constant (J K^{-1}), μ is the air dynamic viscosity (Pa s),

$C_1 = 1 + 0.388\mathrm{Kn}_f\left[(1-\alpha)\mathrm{Pe}/\mathrm{KU}\right]^{1/3}$ and $C_2 = 1/1 + 1.6\left[\left(\frac{1-\alpha}{\mathrm{KU}}\right)\right]^{\frac{1}{3}} \mathrm{Pe}^{-\frac{2}{3}} C1.$

$\mathrm{Kn}_f = 2\lambda/\mathrm{Df}$ is the Knudsen number of the fiber.

The results of filtration efficiency are shown in Fig. 9. The R^2 value was 0.99, which indicates that the calculation results are in good agreement with the measured results.

It is observed that in the particle size range of 100 to 300 nm, the filtration efficiency is a decreasing process in which the diffusion mechanism is dominant. It occurs because air molecules are always in a state of random motion. As air molecules impact particles in the air stream, they move them in different directions, and the movement of contaminants is known as Brownian motion. It is observed that MPPS (maximum penetrating particle size) is present in the 300 nm particle size. As a result, the filtration efficiency at this particle size is

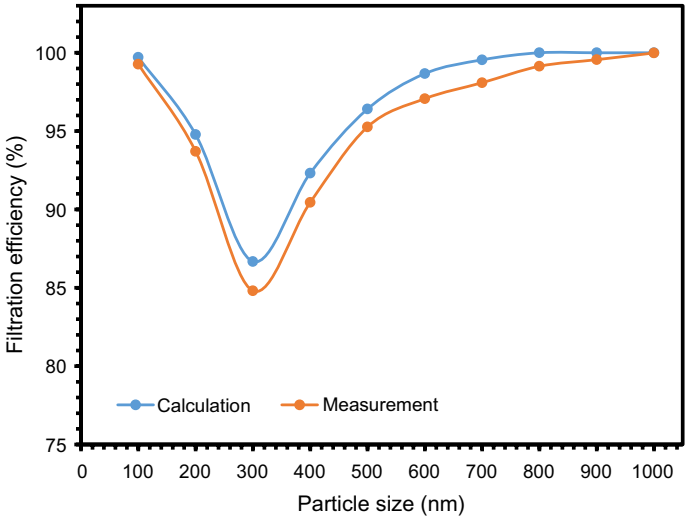

Fig. 9 The filtration efficiency of PAN10%-1%Ag membrane based on measured and calculated results

minimal. Furthermore, at 300–1000 nm particle sizes, the dominant mechanism is the interception. In this mechanism, when the particles are larger than the filter media pore size or flow path, particles are removed by the filter media. Therefore, as the particle size increases, the filtration efficiency increases.

Conclusions

In summary, after trial and error and optimization of conditions, PAN10%-1%Ag membrane with suitable morphology and uniform diameter distribution was successfully designed and fabricated by electrospinning. These electrospun mats showed the good mechanical property and antibacterial activity toward *Staphylococcus aureus* (Gram-positive bacteria) and *Escherichia coli* (Gram-negative bacteria).

With integrated properties of ultrafine diameter, small pore size, high porosity, and high specific surface area, the resulting PA-6 NFN membranes exhibit robust mechanical strength, high filtration efficiency of 99.27% for the 100 nm aerosol particles, less pressure drop of 33 Pa and higher filtration efficiency and higher quality factor for airborne particles compared to the two standard commercial masks including of three-ply surgical mask and respirator face mask. The basis weight of a PAN-Ag nanofiber membrane is only 1.50 g/m^2, 1/54 th of a typical commercial mask with similar filtration efficiency. After 24 h of operation of the filtration process in a simulated living environment, the obtained air filter still displayed a high filtration efficiency and a less variation pressure drop. In addition, the R^2 value was 0.99, which indicates the calculated filtration efficiency results are in good agreement with the measurement results. It is anticipated that the PAN-Ag membranes will have broad applications, including face masks, indoor air filtration and clean room.

Acknowledgements The authors would like to thank the Department of Textile Engineering, the University of Guilan for Equipment support. The researchers are also grateful to Safety and Environmental Laboratory, Nuclear Fuel Cycle School, Nuclear Science and Technology Research Institute for providing their lab facilities for the Filtration Media Quality Test.

Funding The author(s) received no financial support for the research, authorship, and/or publication of this article.

Declarations

Conflict of interest The author(s) declared no potential conflicts of interest with respect to the research, authorship, and/or publication of this article.

References

1. Gu GQ, Han CB, Lu CX, He C, Jiang T, Gao ZL, Li CJ, Wang ZL (2017) Triboelectric nanogenerator enhanced nanofiber air filters for efficient particulate matter removal. ACS Nano 11(6):6211–6217

2. Ding X, Li Y, Si Y, Yin X, Yu J, Ding B (2019) Electrospun polyvinylidene fluoride/SiO_2 nanofibrous membranes with enhanced electret property for efficient air filtration. Compos Commun 13:57–62
3. Kadam V, Truong YB, Easton C, Mukherjee S, Wang L, Padhye R, Kyratzis IL (2018) Electrospun polyacrylonitrile/β-cyclodextrin composite membranes for simultaneous air filtration and adsorption of volatile organic compounds. ACS Appl Nano Mater 1(8):4268–4277
4. Yang X, Pu Y, Li S, Liu X, Wang Z, Yuan D, Ning X (2019) Electrospun polymer composite membrane with superior thermal stability and excellent chemical resistance for high-Efficiency PM2.5 capture. ACS Appl Mater Interfaces 11(46):43188–43199
5. Zhang C, Yao L, Yang Z, Kong ES, Zhu X, Zhang Y (2019) Graphene oxide-modified polyacrylonitrile nanofibrous membranes for efficient air filtration. ACS Appl Nano Mater 2(6):3916–3924
6. Liu G, Xiao M, Zhang X, Gal C, Chen X, Liu L, Pan S, Wu J, Tang L, Clements-Croome D (2017) A review of air filtration technologies for sustainable and healthy building ventilation. Sustain Cities Soc 32:375–396
7. Mamun A, Blachowicz T, Sabantina L (2021) Electrospun nanofiber mats for filtering applications—Technology, structure and materials. Polymers 13(9):1368
8. Wan H, Wang N, Yang J, Si Y, Chen K, Ding B, Sun G, El-Newehy M, Al-Deyab SS, Yu J (2014) Hierarchically structured polysulfone/titania fibrous membranes with enhanced air filtration performance. J Colloid Interface Sci 417:18–26
9. Uppal R, Bhat G, Eash C, Akato K (2013) Meltblown nanofiber media for enhanced quality factor. Fibers Polym 14(4):660–668
10. Xu Z, Zhou B (2014) Fundamentals of air cleaning technology and its application in cleanrooms. Springer, Berlin, pp 560–567
11. Hung CH, Leung WW (2011) Filtration of nano-aerosol using nanofiber filter under low Peclet number and transitional flow regime. Sep Purif Technol 79(1):34–42
12. Wang CS, Otani Y (2013) Removal of nanoparticles from gas streams by fibrous filters: a review. Ind Eng Chem Res 52(1):5–17
13. Mikheev AY, Kanev IL, Morozova TY, Morozov VN (2013) Water-soluble filters from ultra-thin polyvinylpirrolidone nanofibers. J Membr Sci 448:151–159
14. Zhao X, Wang S, Yin X, Yu J, Ding B (2016) Slip-effect functional air filter for efficient purification of PM 2.5. Sci Rep 6(1):35472
15. Li P, Wang C, Zhang Y, Wei F (2014) Air filtration in the free molecular flow regime: a review of high-efficiency particulate air filters based on carbon nanotubes. Small 10(22):4543–4561
16. Tanaka S, Doi A, Nakatani N, Katayama Y, Miyake Y (2009) Synthesis of ordered mesoporous carbon films, powders, and fibers by direct triblock-copolymer-templating method using an ethanol/water system. Carbon 47(11):2688–26898
17. Wang D, Sun G, Chiou BS (2007) A high-throughput, controllable, and environmentally benign fabrication process of thermoplastic nanofibers. Macromol Mater Eng 292(4):407–414
18. Qiu P, Mao C (2010) Biomimetic branched hollow fibers templated by self-assembled fibrous polyvinylpyrrolidone structures in aqueous solution. ACS Nano 4(3):1573–1579
19. Wang X, Li Y (2002) Selected-control hydrothermal synthesis of α-and β-MnO_2 single crystal nanowires. J Am Chem Soc 124(12):2880–2881
20. Podgorski A, Bałazy A, Gradoń L (2006) Application of nanofibers to improve the filtration efficiency of the most penetrating aerosol particles in fibrous filters. Chem Eng Sci 61(20):6804–6815
21. Raghavan P, Lim DH, Ahn JH, Nah C, Sherrington DC, Ryu HS, Ahn HJ (2012) Electrospun polymer nanofibers: the booming cutting edge technology. React Funct Polym 72(12):915–930
22. Liu YP, Deng YB, Jiang ZX (2012) Effect of nanofiber diameter on filtration efficiency. Adv Mater Res 560:737–741
23. Xu N, Cao J, Lu Y (2015) The structure and property evaluation of electrospun porous fibrous membrane based on the copolymer of styrene and butyl acrylate. J Porous Mater 22(6):1539–1548
24. Bhardwaj N, Kundu SC (2010) Electrospinning: a fascinating fiber fabrication technique. Biotechnol Adv 28(3):325–347
25. Sohrabi M, Abbasi M, Ansar MM, Soltani Tehrani B (2021) Evaluation of electrospun nanofibers fabricated using PCL/PVP and PVA/β-TCP as potential scaffolds for bone tissue engineering. Polym Bull 4:1–7
26. Habibi Mohraz M, Golbabaei F, Je YuI, Sedigh Zadeh A, Mansournia MA, Farhang Dehghan S (2018) Investigating effective parameters on the nanoparticles air filtration using Polyurethane nanofiber mats. J Health Safe Work 8(1):29–42

27. Wang J, Zhao W, Wang B, Pei G, and Li C (2017) Multilevel-layer-structured polyamide 6/poly (trimethylene terephthalate) nanofibrous membranes for low-pressure air filtration. J Appl Polym Sci 134(16)
28. Sill TJ, Von Recum HA (2008) Electrospinning: applications in drug delivery and tissue engineering. Biomaterials 29(13):1989–2006
29. Lowe A, Bills J, Verma R, Lavery L, Davis K, Balkus KJ Jr (2015) Electrospun nitric oxide releasing bandage with enhanced wound healing. Acta Biomater 13:121–130
30. MacDiarmid AG, Yang LS, Huang WS, Humphrey BD (1987) Polyaniline: electrochemistry and application to rechargeable batteries. Synth Met 18(1–3):393–398
31. Nisbet DR, Rodda AE, Finkelstein DI, Horne MK, Forsythe JS, Shen W (2009) Surface and bulk characterisation of electrospun membranes: problems and improvements. Colloids Surf B 71(1):1–2
32. Obaid M, Barakat NA, Fadali OA, Motlak M, Almajid AA, Khalil KA (2015) Effective and reusable oil/water separation membranes based on modified polysulfone electrospun nanofiber mats. Chem Eng J 259:449–456
33. Mei Y, Wang Z, Li X (2013) Improving filtration performance of electrospun nanofiber mats by a bimodal method. J Appl Polym Sci 128(2):1089–1094
34. Liu B, Zhang S, Wang X, Yu J, Ding B (2015) Efficient and reusable polyamide-56 nanofiber/nets membrane with bimodal structures for air filtration. J Colloid Interface Sci 457:203–2011
35. Macfarlane AL, Kadla JF, Kerekes RJ (2012) High performance air filters produced from freeze-dried fibrillated wood pulp: fiber network compression due to the freezing process. Ind Eng Chem Res 51(32):10702–10711
36. Khalid B, Bai X, Wei H, Huang Y, Wu H, Cui Y (2017) Direct blow-spinning of nanofibers on a window screen for highly efficient PM2.5 removal. Nano Lett 17(2):1140–1148
37. Kim J, Chan Hong S, Bae GN, Jung JH (2017) Electrospun magnetic nanoparticle-decorated nanofiber filter and its applications to high-efficiency air filtration. Environ Sci Technol 51(20):11967–11975
38. Souzandeh H, Scudiero L, Wang Y, Zhong WH (2017) A disposable multi-functional air filter: paper towel/protein nanofibers with gradient porous structures for capturing pollutants of broad species and sizes. ACS Sustain Chem Eng 5(7):6209–6217
39. Liu C, Hsu PC, Lee HW, Ye M, Zheng G, Liu N, Li W, Cui Y (2015) Transparent air filter for high-efficiency PM 2.5 capture. Nat Commun 6(1):6205
40. Zhang Q, Li Q, Young TM, Harper DP, Wang S (2019) A novel method for fabricating an electrospun poly (vinyl alcohol)/cellulose nanocrystals composite nanofibrous filter with low air resistance for high-efficiency filtration of particulate matter. ACS Sustain Chem Eng 7(9):8706–8714
41. Wang S, Zhao X, Yin X, Yu J, Ding B (2016) Electret polyvinylidene fluoride nanofibers hybridized by polytetrafluoroethylene nanoparticles for high-efficiency air filtration. ACS Appl Mater Interfaces 8(36):23985–23994
42. Balgis R, Murata H, Goi Y, Ogi T, Okuyama K, Bao L (2017) Synthesis of dual-size cellulose–polyvinylpyrrolidone nanofiber composites via one-step electrospinning method for high-performance air filter. Langmuir 33(24):6127–6134
43. Rujitanaroj PO, Pimpha N, Supaphol P (2010) Preparation, characterization, and antibacterial properties of electrospun polyacrylonitrile fibrous membranes containing silver nanoparticles. J Appl Polym Sci 116(4):1967–1976
44. Aragon D, Sole ML, Brown S (2005) Outcomes of an infection prevention project focusing on hand hygiene and isolation practices. AACN Clin Issues 16(2):121–132
45. Xu F, Piett C, Farkas S, Qazzaz M, Syed NI (2013) Silver nanoparticles (AgNPs) cause degeneration of cytoskeleton and disrupt synaptic machinery of cultured cortical neurons. Mol Brain 6(1):1–5
46. Zhang C, Yang Q, Zhan N, Sun L, Wang H, Song Y, Li Y (2010) Silver nanoparticles grown on the surface of PAN nanofiber: preparation, characterization and catalytic performance. Colloids Surf A 362(1–3):58–64
47. Chen Y, Liu HY, Zhang ZJ (2010) Characterization and morphology of composites prepared from polyacrylonitrile and silver nitrate. Appl Mech Mater 26:159–162
48. Sichani GN, Morshed M, Amirnasr M, Abedi D (2010) In situ preparation, electrospinning, and characterization of polyacrylonitrile nanofibers containing silver nanoparticles. J Appl Polym Sci 116(2):1021–1029
49. Xiu ZM, Zhang QB, Puppala HL, Colvin VL, Alvarez PJ (2012) Negligible particle-specific antibacterial activity of silver nanoparticles. Nano Lett 12(8):4271–4275

50. Huang JJ, Tian Y, Wang R, Tian M, Liao Y (2020) Fabrication of bead-on-string polyacrylonitrile nanofibrous air filters with superior filtration efficiency and ultralow pressure drop. Sep Purif Technol 237:116377
51. Li P, Zong Y, Zhang Y, Yang M, Zhang R, Li S, Wei F (2013) In situ fabrication of depth-type hierarchical CNT/quartz fiber filters for high efficiency filtration of sub-micron aerosols and high water repellency. Nanoscale 5(8):3367–33672
52. Wang N, Si Y, Wang N, Sun G, El-Newehy M, Al-Deyab SS, Ding B (2014) Multilevel structured polyacrylonitrile/silica nanofibrous membranes for high-performance air filtration. Sep Purif Technol 126:44–51
53. Al-Attabi R, Morsi Y, Kujawski W, Kong L, Schütz JA, Dumée LF (2019) Wrinkled silica doped electrospun nano-fiber membranes with engineered roughness for advanced aerosol air filtration. Sep Purif Technol 215:500–507
54. Zhou X, Luo Z, Tao P, Jin B, Wu Z, Huang Y (2014) Facile preparation and enhanced photocatalytic H2-production activity of Cu $(OH)_2$ nanospheres modified porous g-C_3 N_4. Mater Chem Phys 143(3):1462–1468
55. Li B, Cao H, Shao J, Qu M (2011) Enhanced anode performances of the Fe_3O_4–Carbon–rGO three dimensional composite in lithium ion batteries. Chem Commun 47(37):10374–10376